

Continued fraction solution to the Raman interaction of a trapped ultracold ion with two traveling wave lasers

Mang Feng

¹*Max-Planck Institute for the Physics of Complex Systems,
Nöthnitzer Street 38, 01187 Dresden, Germany*

²*Laboratory of Magnetic Resonance and Atomic and Molecular Physics,
Wuhan Institute of Physics and Mathematics, Academia Sinica,
Wuhan 430071 People's Republic of China*

(November 23, 2018)

Abstract

Raman interaction of a trapped ultracold ion with two traveling wave lasers has been used extensively in the ion trap experiments. We solve this interaction in the absence of the rotating wave approximation by a continued fraction, without considering the restriction of the Lamb-Dicke limit and the weak excitation regime. Some interesting characteristics of the ion-trap system, particularly for the ion outside the weak excitation regime are found. Finally, a comparison of our results with the solution under the rotating wave approximation is made.

PACS numbers: 42.50.DV, 32.60.+i

Typeset using REVTeX

Quantum effects in the motion of trapped ultracold ions have been drawn much attention in recent years since the success that a single ultracold ion was confined in the ground state of a Paul trap^[1]. Considerable progress has been made so far, such as the preparation and measurement of various nonclassical states^[2], and two qubits logic gate operation^[3], which are of great current interest in ion trap experiment.

It has been proven that a trapped ultracold ion experiencing laser waves can be described by the Jaynes-Cummings model(JCM)^[4] under the rotating wave approximation(RWA). The JCM, describing a two-level system coupled to a harmonic oscillator under RWA in the case of near resonance and weak coupling, has successfully dealt with the cavity QED problems, in which a two-level atom interacts with a monochromatic cavity mode with the form of harmonic oscillator. In the trapped ion configuration, the ion is simplified to be two levels and supposed to move within the region of the space much smaller than the effective wavelength of the laser wave(Lamb-Dicke limit), the vibrational level of the trap is quantized as the harmonic oscillator, and the laser radiating the ion is generally supposed as the classical form of a standing or traveling wave. Different from the situation of cavity QED, the strength of the coupling between the ion and the oscillator can be conveniently adjusted simply by changing the intensity of the laser. For example, in the strong excitation regime^[5,6,8], the coupling constant, denoted by Rabi frequency, is larger than the trapping frequency, which makes RWA no longer valid.

Under RWA, along with the assumption that the ion is confined within the Lamb-Dicke limit(LDL) and weak excitation regime(i.e., the Rabi frequency being smaller than the trapping frequency), one may easily obtain three simple cases^[4,6], that is, carrier excitation, red detuning and blue detuning. If excluding the supposition with respect to the LDL and weak excitation regime, Vogel and his coworkers gave a standard approach to such a nonlinear JC model^[7]. However, in case the RWA is excluded, the ion trap problem turns to be non-integrable, whose solutions have to be obtained completely by the numerical calculation^[6,8]. Recently, we analytically treated^[9] the interaction in the absence of RWA between a standing wave laser and a trapped ultracold ion in coherent state representation^[10,11]. Although

those analytical results are only some particular solutions to the problem, some important information neglected in former works due to use of RWA were presented. However, our investigation in that work was only under both the weak excitation regime and the LDL. Moreover, the solutions in that work strongly depended on the truncation of the series, and thereby the deduction and the forms of the analytical expressions went tedious with the increase of the number of terms in the series, which makes it hard to obtain the eigenenergies and eigenfunctions rapidly at our disposal. Furthermore, it is Raman configurations that are usually applied in actual ion trap experiments for the interaction between lasers and ions, instead of the simple case described in Ref.[9]. Therefore, in this contribution, we choose Raman Λ -type configuration (shown in Fig.1) for a study, which corresponds to the actual process in the NIST experiments^[1]. To present a more general description for such a model, we will exclude the assumption related to both the weak excitation regime and LDL by means of some unitary transformations. Moreover, to overcome the difficulty of complicated analytical deduction, our solution will resort to a continued fraction, from which the eigenenergies of the system and the coefficients of the series of the eigenfunctions can be rapidly obtained by numerical calculation.

Fig.1 describes the interaction of a trapped ultracold ion with two off-resonant counter-propagating traveling wave lasers with frequencies ω_1 and ω_2 respectively. Both laser beams are assumed to propagate along the x axis, and the problem is thereby one-dimensional. For a sufficiently large detuning δ , the third level $|r\rangle$ may be adiabatically eliminated, and we face an effective two-level system, in which the lasers drive the electric-dipole forbidden transition $|g\rangle \leftrightarrow |e\rangle$. In the frame rotating with the effective laser frequency $\omega_L (= \omega_1 - \omega_2)$, the dimensionless Hamiltonian of this system is^[1,2,12]

$$H = \frac{\Delta}{2}\sigma_z + a^\dagger a + \frac{\Omega}{2}(\sigma_+ e^{i\eta\hat{x}} + \sigma_- e^{-i\eta\hat{x}}) \quad (1)$$

where $\Delta = (\omega_0 - \omega_L)/\nu$ with ω_0 being the resonant frequency of the two levels of the ion, and ν being the trap frequency. Ω is the dimensionless Rabi frequency and η the Lamb-Dicke parameter. σ_i ($i = \pm, z$) are Pauli operators, $\hat{x} = a^\dagger + a$ is the dimensionless

position operator of the ion with a^+ and a being operators of creation and annihilation of the phonon field, respectively. The notations '+' and '-' in front of $i\eta\hat{x}$ indicate that the laser wave propagates towards x and $-x$ directions, respectively. ν is generally supposed to be much greater than the atomic decay rate (strong confinement limit) for neglecting the effect of the atomic decay.

We first perform some unitary transformations on Eq.(1)^[12], and obtain

$$H^I = UHU^+ = \frac{\Omega}{2}\sigma_z + a^+a + g(a^+ + a)(\sigma_+ + \sigma_-) + \epsilon(\sigma_+ + \sigma_-) + g^2 \quad (2)$$

where $U = \frac{1}{\sqrt{2}}e^{i\pi a^+a/2} \begin{pmatrix} D^+(\beta) & D(\beta) \\ -D^+(\beta) & D(\beta) \end{pmatrix}$ with $D(\beta) = e^{i\eta(a^++a)/2}$, $g = \eta/2$ and $\epsilon = -\Delta/2$. Comparing with Ref.[9], Eq.(2) can be regarded mathematically as the simplified form of Eq.(6) in Ref.[9] without the two-phonon processes, whereas the optical resonance frequency is replaced by the Rabi frequency. Similar to Ref.[9], we set $a^+ \rightarrow \alpha$, $a \rightarrow \frac{d}{d\alpha}$, and rewrite Eq.(2) in coherent state representation, that is,

$$H = \frac{\Omega}{2}\sigma_z + \alpha\frac{d}{d\alpha} + g(\alpha + \frac{d}{d\alpha})(\sigma_+ + \sigma_-) + \epsilon(\sigma_+ + \sigma_-) + g^2 \quad (3)$$

where α is a complex number and $\int \frac{d\alpha d\alpha^*}{2\pi i} \exp(-|\alpha|^2)|\alpha^* \rangle \langle \alpha^*| = 1$. The eigenfunction of the Schrödinger equation of Eq.(3) can be supposed to be $\Psi(\alpha) = \begin{pmatrix} \Psi_1(\alpha) \\ \Psi_2(\alpha) \end{pmatrix}$, and the eigenenergy is E . Thus we have

$$(\alpha + g)\frac{d}{d\alpha}\Phi_1 = (E - g^2 - g\alpha - \epsilon)\Phi_1 - \frac{\Omega}{2}\Phi_2, \quad (4)$$

$$(\alpha - g)\frac{d}{d\alpha}\Phi_2 = (E - g^2 + g\alpha + \epsilon)\Phi_2 - \frac{\Omega}{2}\Phi_1 \quad (5)$$

where we have made a transformation $\Phi_1 = \Psi_1(\alpha) + \Psi_2(\alpha)$ and $\Phi_2 = \Psi_1(\alpha) - \Psi_2(\alpha)$. To solve Eqs.(4) and (5), we order $\xi = \alpha + g$, and $\Phi_1 = \exp(-g\xi)\phi(\xi)$. Combining Eq.(4) with Eq.(5) will yield a second-order differential equation

$$\begin{aligned} \xi(\xi - 2g)\frac{d^2}{d\xi^2}\phi + [2gE - 2g - 2g\epsilon + (1 + 4g^2 - 2E)\xi - 2g\xi^2]\frac{d}{d\xi}\phi + \\ [E^2 - \epsilon^2 - \frac{\Omega^2}{4} - 4g^2E + 4g^2\epsilon + 2g(E - \epsilon)\xi]\phi = 0. \end{aligned} \quad (6)$$

By supposing ϕ to be a series form $\phi = \sum_{n=0}^{\infty} C_n \xi^n$, Eq.(6) becomes a recurrence relation about the coefficient C_n

$$\alpha_n C_{n+1} + \beta_n C_n + \gamma_n C_{n-1} = 0 \quad (7)$$

where $\alpha_n = 2g(n+1)(E - \epsilon - 1 - n)$, $\beta_n = [n^2 + 2n(2g^2 - E) + E^2 - \epsilon^2 - \frac{\Omega^2}{4} - 4g^2 E + 4g^2 \epsilon]$ and $\gamma_n = 2g(E - \epsilon - n + 1)$. Obviously, by cutting the series at $C_{-1} = 0$, we have $C_1/C_0 = -\beta_0/\alpha_0$, and other coefficients $C_n (n = 2, 3, \dots)$ will be denoted by C_0 . Making a slight transformation for Eq.(7), we obtain following continued fraction,

$$\beta_n - \frac{\gamma_n \alpha_{n-1}}{\beta_{n-1} - \frac{\gamma_{n-1} \alpha_{n-2}}{\beta_{n-2} - \dots \frac{\gamma_2 \alpha_1}{\beta_1 - \gamma_1 \alpha_0 / \beta_0}}} = \frac{\alpha_n \gamma_{n+1}}{\beta_{n+1} - \frac{\alpha_{n+1} \gamma_{n+2}}{\beta_{n+2} - \dots \frac{\alpha_{n+2} \gamma_{n+3}}{\dots}}} \quad (8)$$

from which the eigenenergies E can be easily obtained, and the coefficients $C_n (n = 1, 2, \dots)$ can also be solved^[13].

Prior to the numerical calculation for Eq.(8), we first consider a special case of the problem, that is, the case of LDL and large detuning in the strong excitation regime. At this time, Eq.(3) reduces to the mathematical form similar to the carrier excitation, i.e., $H = \frac{\Omega}{2} \sigma_z + \alpha \frac{d}{d\alpha} + \epsilon(\sigma_+ + \sigma_-)$. With above procedure, we can obtain

$$\beta_n = 0 \implies E = n \pm \sqrt{\frac{\Omega^2}{4} + \epsilon^2}$$

which is in good agreement with the solution in Fock state representation. Except for this special case, the other situations of the problem have to be solved numerically from Eq.(8). Obviously, the convergence of the coefficients C_n is the necessary condition in the calculation. As this condition has been discussed in Ref.[13], we will not repeat it here. The numerical calculation of Eq.(8) demonstrated in Figs.2,3 and 4 may present us following interesting results:

- (i) the eigenenergies of the system increase with the enhancement of Ω and η , which means that it is more difficult to stably confine the ultracold ion outside the LDL and weak excitation regime;
- (ii) the increase of the eigenenergies with the enhancement of η is suppressed by the large

detunings. In view of physics, the only reasonable explanation for this case is that the interaction between the laser and the ion plays main role in the system. With the increase of the detuning, this interaction goes weaker and weaker. Therefore, although the energy of the ion itself is enhanced with the increase of η , the energy of the total system remains nearly constant;

(iii) Fig.4 presents the relation between Ω and Δ for certain values of E and η . From the forms of the curves, we may guess that the relation among E , Δ , η and Ω is of the form of $\Omega = f(E)[1 - h(\eta)\Delta^2]$ with $f(E)$ and $h(\eta)$ being positive definition functions of E and η , respectively.

Moreover, from the specific calculation, we found that, for a certain Ω , with the increase of η , the convergence of C_n would get worse and worse, particularly for the large detuning case. But the larger the value of Ω , the larger the value of η for satisfying the convergence of C_n . The problem with respect to the convergence will be discussed physically later.

Returning Eqs.(4) and (5), we can find that $\Phi_1 = \exp(g\xi)\phi$ is another solution for $\xi = \alpha + g$. Repeating above deduction, we will obtain Eq.(8), whereas in this case, $\alpha_n = 2g(n+1)(E-1-\epsilon-n)$, $\beta_n = (n^2 - 2nE - 4ng^2 + E^2 - \epsilon^2 - \frac{\Omega^2}{4} - 4g^2)$ and $\gamma_n = 2g(n-\epsilon-E)$. Similar to above procedure, we studied the relation among E , Δ , Ω and η , as shown in Figs.5, 6 and 7. Comparing with Figs.2, 3 and 4 respectively, we may find that the values in Figs.5, 6 and 7 are slightly different, and their difference become more and more obvious with the increase of η and Ω , or E and η . Particularly for the case of $\Omega = 2$ and $\Delta = 2.0$ in Fig. 6, the curve no longer upgrades with the increase of η .

As we obtained the solutions of Φ_1 , Φ_2 can be easily solved from Eqs.(4) and (5) with the form of $\Phi_2 = -\frac{2}{\Omega} \sum_{n=0}^{\infty} (n-E+\epsilon)C_n(\alpha+g)^n e^{\pm g(\alpha+g)}$. Therefore, the eigenfunction of the system is

$$\Psi(\alpha) = \begin{pmatrix} \Psi_1(\alpha) \\ \Psi_2(\alpha) \end{pmatrix} = \frac{1}{2} e^{\pm g(\alpha+g)} \begin{pmatrix} \sum_{n=0}^{\infty} C_n [1 - \frac{2}{\Omega}(n-E+\epsilon)] (\alpha+g)^n \\ \sum_{n=0}^{\infty} C_n [1 + \frac{2}{\Omega}(n-E+\epsilon)] (\alpha+g)^n \end{pmatrix} \quad (9)$$

From Refs.[9,10,15], we know that the coherent states can be conveniently transformed to the Fock states with the formula

$$|n \rangle = \int \frac{d\alpha d\alpha^*}{2\pi i} \exp(-|\alpha|^2) |\alpha^* \rangle \frac{1}{\sqrt{n!}} \alpha^n. \quad (10)$$

By means of Baker-Campbell-Hausdorff formula, we may find $e^{g\alpha}\alpha^n$ in coherent state representation correspond to the displaced Fock state $|n, g \rangle$. Therefore, $\Psi(\alpha)$ in Eq.(9) is in fact a superposition of several displaced Fock states. However, to obtain the eigenfunctions in the original representation, we should consider the transformation made in Eq.(2). As an example, we may treat the special case $H = \frac{\Omega}{2}\sigma_z + \alpha \frac{d}{d\alpha} + \epsilon(\sigma_+ + \sigma_-)$, whose eigenfunction is

$$\Psi^S(\alpha) = \begin{pmatrix} \Psi_1^s(\alpha) \\ \Psi_2^s(\alpha) \end{pmatrix} = \frac{1}{2} \begin{pmatrix} A \\ B \end{pmatrix} \sum_{n=0}^{\infty} C_n \alpha^n \quad (11)$$

where $A = 1 \pm \frac{2}{\Omega} \sqrt{\frac{\Omega^2}{4} + \epsilon^2} + \frac{2\epsilon}{\Omega}$, $B = 1 \mp \frac{2}{\Omega} \sqrt{\frac{\Omega^2}{4} + \epsilon^2} + \frac{2\epsilon}{\Omega}$. Then the eigenfunction in the original representation is

$$\begin{aligned} \Psi^{SO}(\alpha) &= \frac{1}{\sqrt{2}} e^{i\pi a^+ a/2} \begin{pmatrix} 1 & 1 \\ -1 & 1 \end{pmatrix} \frac{1}{2} \begin{pmatrix} A \\ B \end{pmatrix} |n \rangle \\ &= \frac{1}{\sqrt{2}} e^{in\pi/2} \begin{pmatrix} 1 + \frac{2\epsilon}{\Omega} \\ \pm \frac{2}{\Omega} \sqrt{\frac{\Omega^2}{4} + \epsilon^2} \end{pmatrix} |n \rangle \end{aligned} \quad (12)$$

where we have made α^n to be Fock state $|n \rangle$ by means of Eq.(10), and simply chosen the coefficients related to α^n to be 1 and $\alpha^m (m \neq n)$ to be zero. From above equation we know that, in the weak excitation regime $\Omega \ll \epsilon$, or in the carrier excitation, i.e., $\epsilon = 0$, $\Psi^{SO}(\alpha) \propto \begin{pmatrix} 1 \\ \pm 1 \end{pmatrix} |n \rangle$, which is identical to the standard solution from Fock state representation^[6]. In general, in the strong excitation regime with large detuning, the probability amplitudes of up and down states will be different, as shown in Eq.(12).

As referred to previously, the problem of eigenfunction and eigenenergy for a trapped and radiated ion was treated numerically in Ref.[6], in which the Hamiltonian was diagonalized in the space spanned by the dressed Fock states. As the solutions of the non-RWA JC model are with the forms of coherent states or squeezed states, etc^[9,14,15], the accurate eigenenergies and eigenfunctions in Ref.[6] might not be in principle solved unless the space for diagonalization was spanned by the infinite dressed Fock states, particularly in the case of the large detuning and strong excitation regime. That is the reason why Ref.[6] only

presented the solutions in the weak excitation regime for the case of near-resonance. In our treatment, however, the numerical solution is made based on the continued fraction, which is obtained in the coherent state representation. So our solution is still valid even for the large detuning and strong excitation regime.

Before ending our discussion, it is interesting to make a comparison between our solution with those under RWA. In general, we may solve Eq.(1) by means of nonlinear JC model as proposed in [7] for the ion governed outside the weak excitation regime. However, to make the comparison easily and obviously, we start our comparison procedure from Eq.(2). By performing a unitary transformation $\exp[-i(\frac{\Omega}{2}\sigma_z + \frac{a+a}{2})t]$ on Eq.(2), we can obtain $E_n^\pm = \frac{2n+1}{4} + \frac{1}{4}\eta^2 \pm \frac{1}{4}\sqrt{4\eta^2(n+1) + 1}$ ($n = 0, 1, 2, \dots$) in the Fock state representation for $\Omega = 2$ under RWA(see Figs.8). From Figs.3, 6 and 8, we see that, for small values of η , the case of $n = 2$ under RWA is similar to those of $\Omega = 2$ in Figs.3 and 6, where E_n^+ and E_n^- are similar respectively to the very large and zero detuning cases without RWA. Although both the solutions with RWA and without RWA include multi-curve, the difference is obvious: as it is merely a particular solution, the solution without RWA approaches to the solution of a certain excited state under RWA. On the other hand, as RWA merely retains some resonance terms in Hamiltonian, the solution under RWA is irrelative to the variation of Δ and just related to a specific value of Ω . Moreover, as they are obtained from the solution of Eq.(8), the results without RWA are restricted by the convergence of the coefficients of the series. In contrast, there is no restriction mathematically for the expressions of the solution under RWA even in the case of $\eta \rightarrow \infty$. However, in physics, η is impossible to approach to infinity for a ultracold ion system, and it must be cut off at a certain value. Therefore, in this sense, the convergence condition in our solution of the continued fraction provides a physical restriction on the final results, which plays the same role as the restricted condition for the solutions in Ref.[9]. Furthermore, further deduction with the transformations $\exp[-i(\frac{\Omega}{2}\sigma_z + \frac{a+a}{4})t]$ and $\exp[-i(\frac{\Omega}{2}\sigma_z + \frac{a+a}{6})t]$ performed on Eq.(2) respectively can tell us that, with the increase of Ω and η , the difference between the solutions with RWA and without RWA will be larger and larger.

In summary, we have presented a continued fraction solution to a trapped and laser-radiated ultracold ion experiencing two traveling wave lasers in a Raman process in the absence of RWA. Instead of the complicated and tedious analytical forms in Ref.[9], we can solve the problem rapidly from the continued fraction and present more complete information of the system, such as the relation among E , Ω , Δ and η . As limitation of weak excitation regime and LDL as well as RWA is excluded in our treatment, our solution is not only exact, but more general. It can be used to investigate quantum properties of the ion-trap system in a wider range of parameters, and serve as a comparison with other approximate works, as we did in Ref.[16]. However, as Eq.(2) represents a kind of typical non-integrable system, our solutions are still only some particular ones. While in comparison with former solutions under RWA, we still found some interesting results, particularly for the case outside the weak excitation regime and LDL. We should emphasize that, it is hard to carry out the trapped ion-laser interaction experimentally outside the weak excitation regime at present due to the requirement of very high intensity of the laser, and the laser cooling to the ground state of the trapping potential has not been reported yet in this regime. Therefore, we hope the solution in our work would be helpful for the future exploration of the quantum properties of the ion-trap system in this respect.

The work is partly supported by National Natural Science Foundation of China under Grant No. 19904013.

Note added: after accomplishing this paper, the author becomes aware of that a work^[17] related to the fast quantum gate for cold trapped ions has been carried out based on Ref.[12] and the treatment similar to our RWA treatment.

REFERENCES

- [1] Diedrich F, Bergquist J C, Itano W M, and Wineland D J, Phys.Rev.Lett. **62** (1989) 403; Monroe C, King B E, Jefferts S R, Itano W M, Wineland D J, Gould P, Phys.Rev.Lett. **75**(1995)4011.
- [2] Meekhof D M, Monroe C, King B E, Itano W M, Wineland D J, Phys.Rev.Lett. **76**(1996)1796; Monroe C, Meekhof D M, King B E and Wineland D J, Science, **272**(1996)1131.
- [3] Monroe C, Meekhof D M, King B E, Itano W M, Wineland D J, Phys.Rev.Lett. **75**(1995)4714.
- [4] Jaynes E T and Cummings F W, Proc.IEEE, **51**(1963)89; Blockley C A, Walls D F, Risken H, Europhys.Lett. **17**(1992)509; Cirac J I, Parkins A S, Blatt R, and Zoller P, Phys.Rev.Lett.**70** (1993)556; Opt.Comm. **97**(1993)353; Cirac J I, Blatt R, Parkins A S, and Zoller P, Phys.Rev.Lett. **70**(1993)762.
- [5] Poyatos J F, Cirac J I, Blatt R and Zoller P, Phys.Rev.A**54**(1996)1532.
- [6] Cirac J I, Parkins A S, Blatt R, and Zoller P, Adv.Atom.Mole. Opti.Phys. V**37**(1996)237.
- [7] Vogel W and Filho R L de M, Phys.Rev.A **52**(1995)4214; Filho R L de M and Vogel W, Phys.Rev.Lett., **76**(1996)608.
- [8] Zeng H, Lin F, Wang Y and Segawa Y, Phys.Rev.A **59**(1999)4589.
- [9] Feng M, Zhu X, Fang X, Yan M and Shi L, J.Phys.B**32** (1999)701.
- [10] Negele J W and Orland H, Quantum Many-Particle Systems (Addison-Wesley, Reading, 1987)20.
- [11] Kuš M and Lewenstein M, J.Phys.A**19** (1986)305.
- [12] Moya-Cessa H, Vidiella-Barranco A, Roversi J A, Freitas D S and Dutra S M, Phys.Rev.A**59**(1999)2518

- [13] Feng M, Fang X, Duan Y, Zhu X, and Shi L, Phys.Lett.A**244** (1998)18.
- [14] Plata J and Llorente J M G, Phys.Rev.A**48**(1993)782.
- [15] Feng M, Fang X, Shi L, Zhu X and Yan M, Commun.Theor.Phys. **31**(1999)175.
- [16] Qin G, Wang K, Li T, Han R and Feng M, Phys.Lett.A**239**(1998)272.
- [17] Jonathan D, Plenio M B and Knight P L, Phys.Rev.A**62**,(2000)042307

Captions of the figures

Fig.1 Level scheme of the internal structure of the trapped ultracold ion, where $|g\rangle \leftrightarrow |e\rangle$ is dipole forbidden.

Fig.2 Variation of E with respect to Δ in the case of $\Phi_1 = \exp(-g\xi)\phi$, where the dotted, dashed, solid and dash-dotted curves represent $\eta = 0.2, 0.4, 0.6$ and 0.8 , respectively. For clarity of the figure, we only plot the cases for $\Omega = 2, 4$ and 6 .

Fig.3 Variation of E with respect to η in the case of $\Phi_1 = \exp(-g\xi)\phi$, where the solid, dotted, dash-dotted and dashed curves represent $\Delta = 0.2, 1.6, 2.0$ and 3.0 , respectively. For clarity of the figure, we only plot the cases for $\Omega = 2, 4$ and 6 .

Fig.4 Variation of Ω with respect to Δ in the case of $\Phi_1 = \exp(-g\xi)\phi$, where the solid, dashed and dotted curves represent $\eta = 0.02, 0.4$ and 0.6 , respectively. We only plot the cases for $E = 3$ and 5 .

Fig.5 Variation of E with respect to Δ in the case of $\Phi_1 = \exp(g\xi)\phi$. The rest are the same as that in Fig.2.

Fig.6 Variation of E with respect to η in the case of $\Phi_1 = \exp(g\xi)\phi$. The rest are the same as that in Fig.3.

Fig.7 Variation of Ω with respect to Δ in the case of $\Phi_1 = \exp(g\xi)\phi$. The rest are the same as that in Fig.4.

Fig.8 Variation of E_n^\pm with respect to η for $\Omega = 2$ for the solution under RWA. See text.

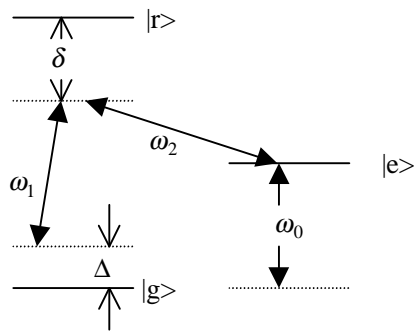


Fig.1

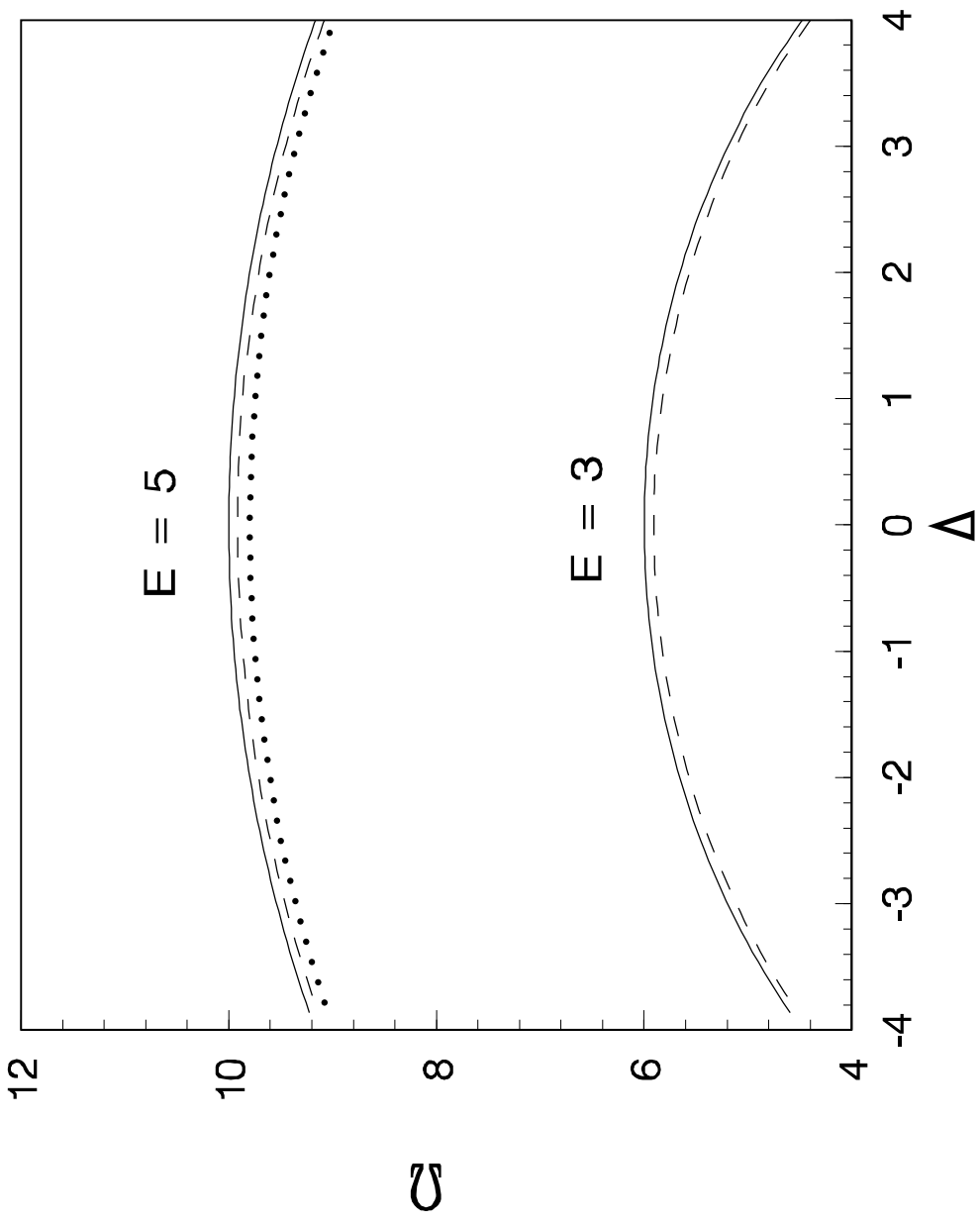


Fig.4

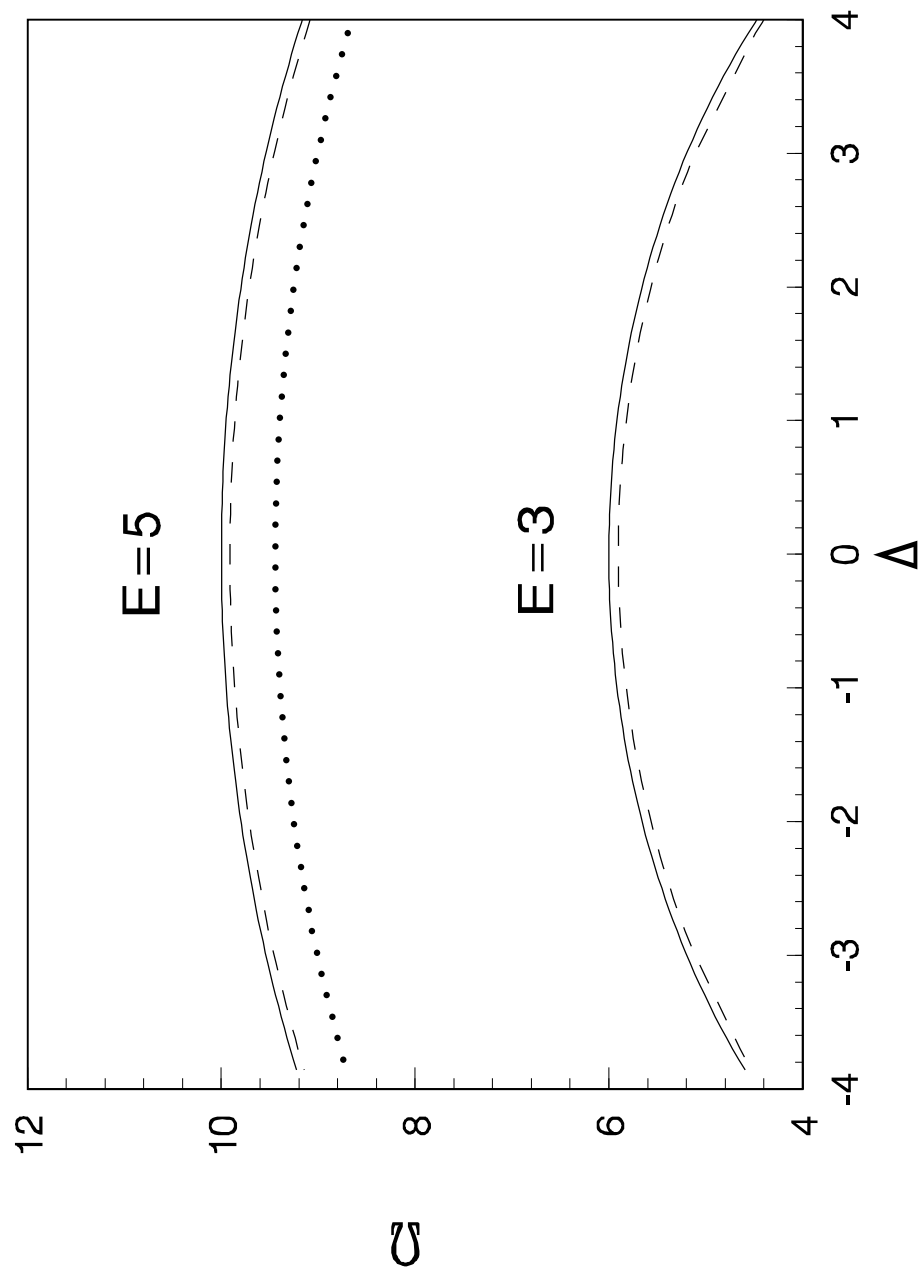


Fig.7

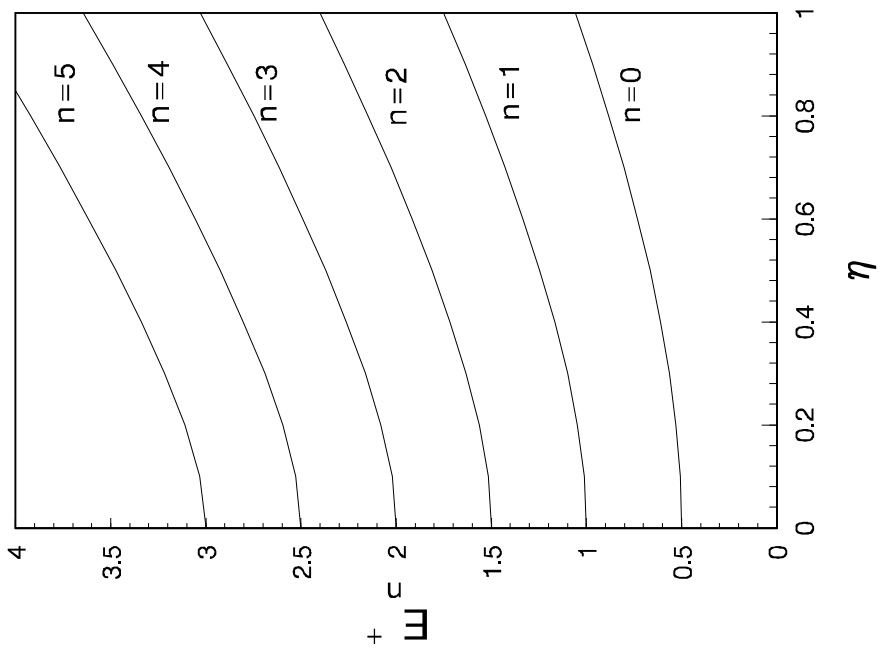
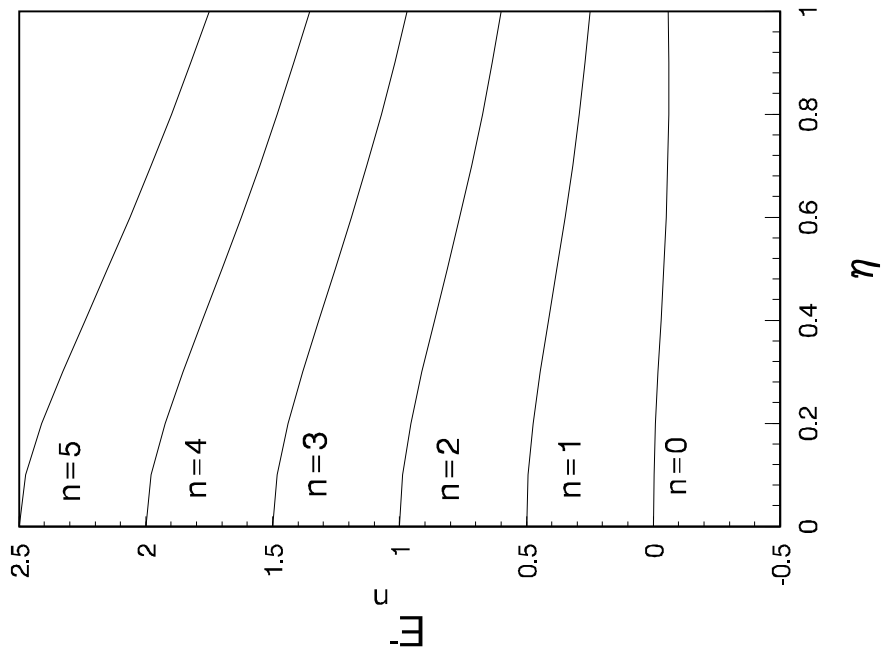


Fig.8

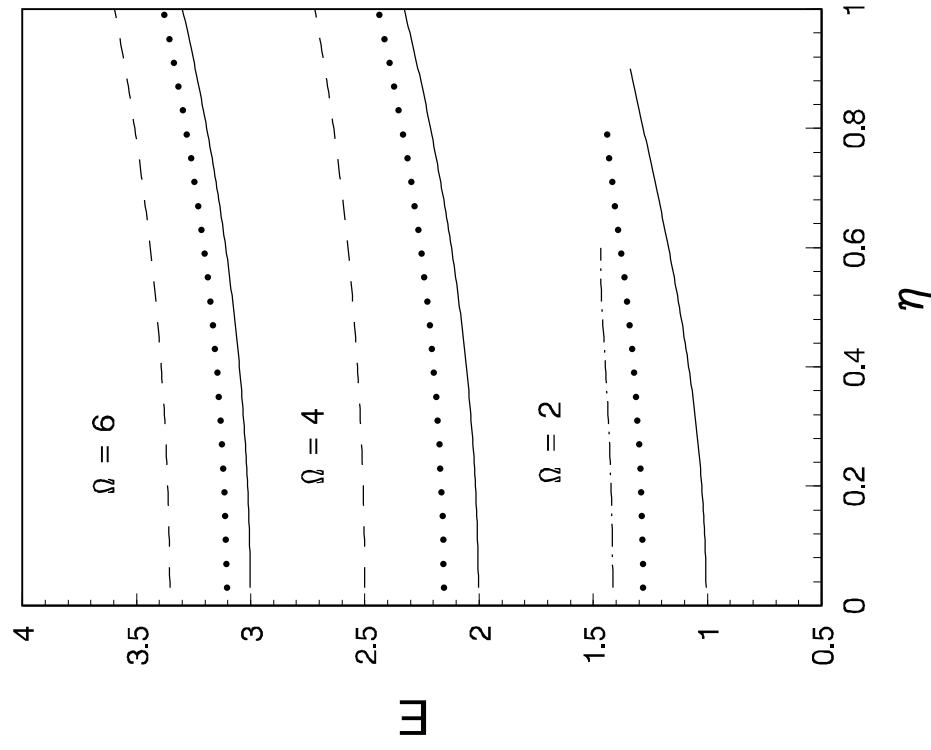


Fig.2

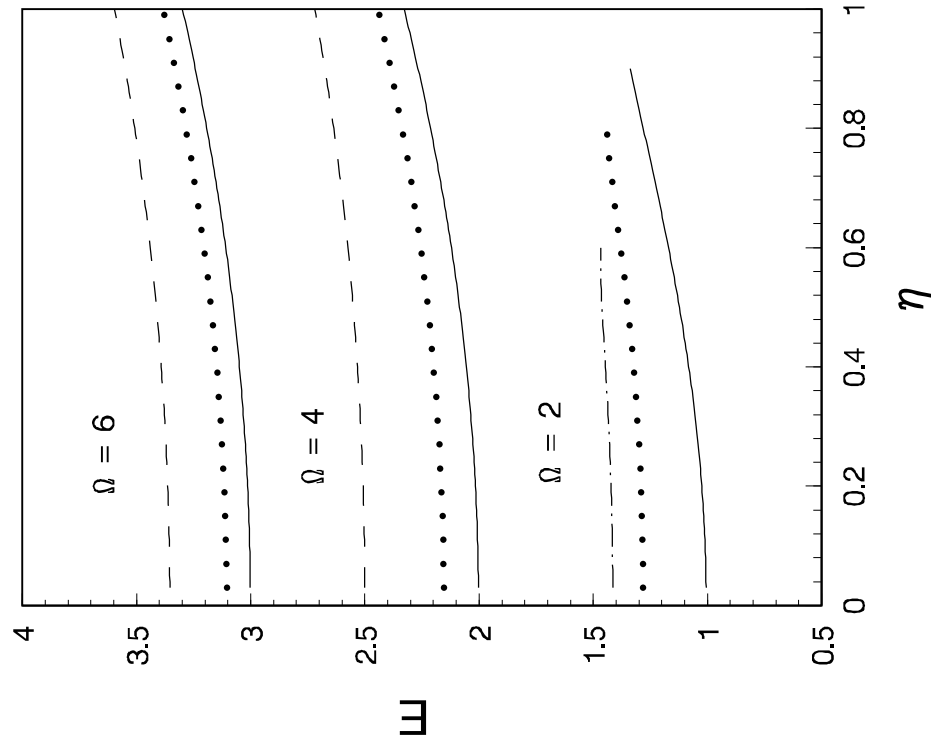


Fig.3

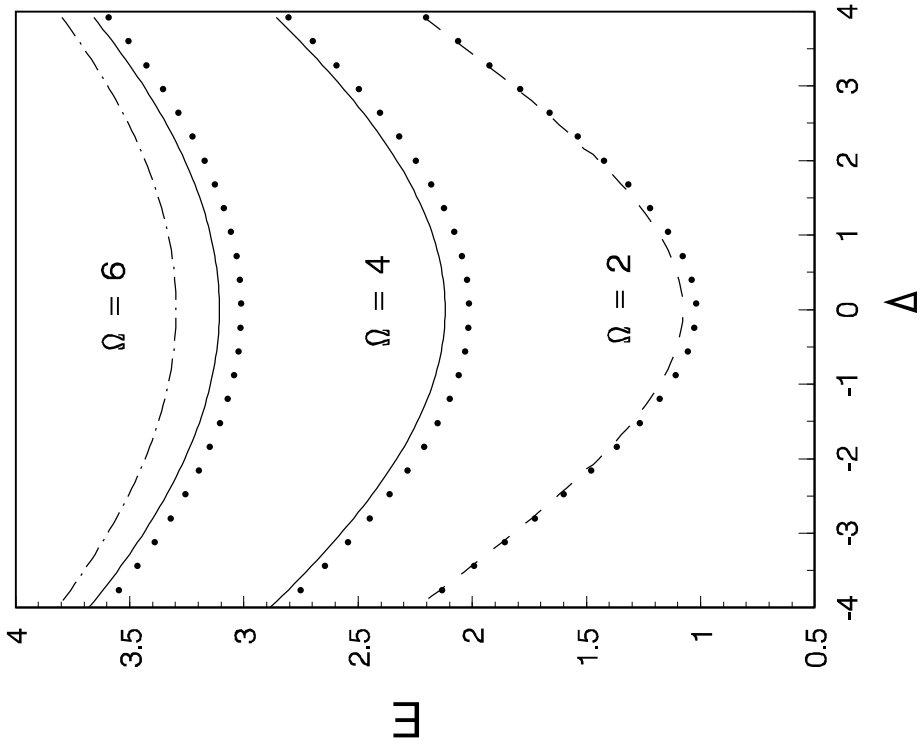


Fig.5

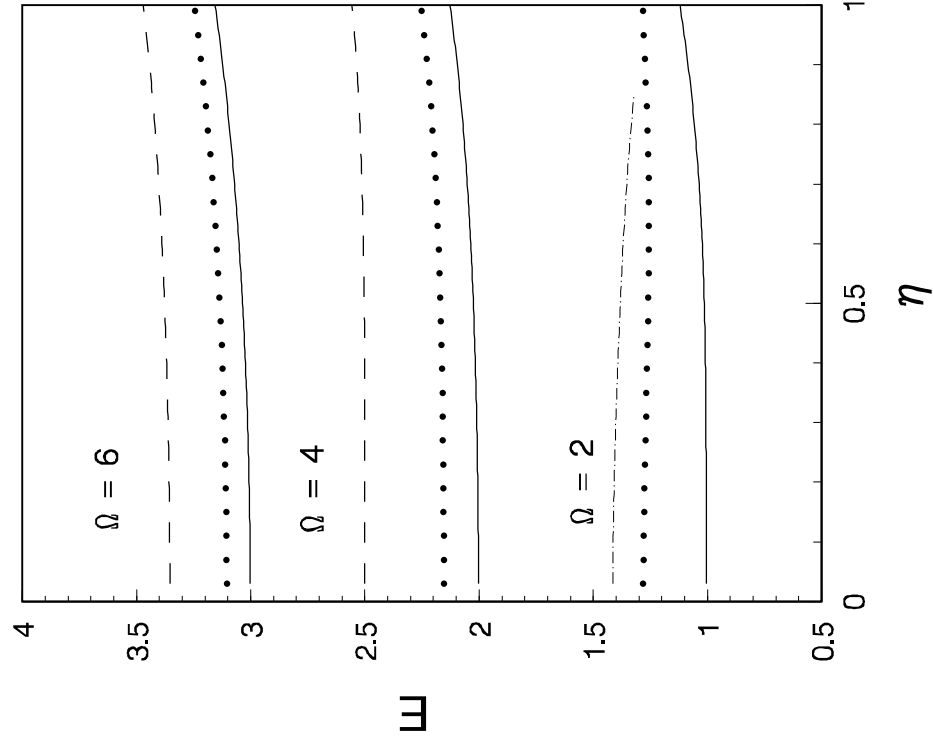


Fig.6